ELSEVIER

Powder Technology 85 (1995) 203–219

POWDER TECHNOLOGY

Pneumatic conveying of ice particles through mine-shaft pipelines

T.J. Sheer

School of Mechanical Engineering, University of the Witwatersrand, Johannesburg, Wits 2050, South Africa

Received 5 September 1994; revised 26 June 1995; accepted 4 July 1995

Abstract

A pilot-plant experimental investigation is described into the pneumatic conveying of large ice particles through long pipelines extending down deep mine shafts. Using low-pressure plastic piping with an inner diameter of 136 mm and cylindrical ice particles with initial dimensions of up to 34 mm, the main testing programme encompassed ice flow rates of up to 7.4 kg/s through a pipeline 2968 m long and extending to a depth of 1770 m below the surface. Ice was also delivered to a depth of 2407 m below the surface through a pipeline 3905 m long. Various regimes of two-phase flow were observed in the various vertical and horizontal sections of the pipeline, including dilute-phase flow and cohesive plug flow. Equations are presented for the prediction of pressure gradients along the respective sections, with empirical correlations for solids friction factors. The investigation proved the feasibility of conveying ice underground for mine-cooling purposes.

Keywords: Pneumatic conveying; Ice particles; Mine shafts; Pipelines

1. Introduction

In very deep mines, such as the gold mines of the Witwatersrand, the greatest challenge in maintaining satisfactory thermal environmental conditions for mining personnel is the removal to the Earth's atmosphere of the heat that flows into the underground working areas. Heat removal systems incorporating refrigeration machines and air-to-water heat exchangers are used, together with the mine ventilation systems to this end. The current practice in many deep mines is to use water, chilled in refrigeration installations located on the surface, as the primary coolant between the underground and surface levels. This water is piped underground and distributed to air coolers and stope faces throughout the mine. After absorbing heat, all this water must be pumped back to the surface and the high associated costs, even if energy-recovery turbines are included in the down-going pipelines, are a major disadvantage.

An attractive concept for reducing the coolant pumping costs is to employ a coolant that undergoes a phase change within the circuit. The particular option described here is to send ice to underground melting chambers to absorb the heat load and to pump the resulting warm water back to the surface. The latent heat of fusion of ice is sufficiently large to allow a reduction in water pumping rate to one-fifth of that in a conventional system, for the same heat removal rate.

At the outset of this investigation it was recognized that the greatest engineering uncertainty concerned the method of transporting the ice underground in large quantities. A typical mine shaft could consume 43 kg/s of ice (3700 tons/day), giving some 18 MW of underground cooling [1]. The ice would be in particulate form, as produced by commercially available ice makers [2]. Pipeline conveying was chosen for evaluation, with air as the conveying medium [3]. This choice was made because of the tortuous nature of the path from the surface to the underground melting chambers, incorporating long successive vertical and horizontal conveying distances. Preliminary investigations indicated a lack of fundamental pneumatic-conveying information relevant to this combination of an unusual conveyed product and an unusual conveying route. A particular concern was the possibility of pipeline blockages, especially at bends following vertical sections.

The literature on pneumatic conveying shows clearly that it remains a necessary practice, when designing conveying systems for any 'new' material, to carry out pilot tests. Because of the complex nature of gas–solid flow in pipes, scaling-up procedures are notoriously unreliable and all experimental work needs to be carried out on test facilities of realistic size. The Chamber of Mines of South Africa accordingly decided to construct a pilot ice-conveying installation, with the objectives of investigating the feasibility of the concept and of formulating design guidelines for future full-scale systems. This paper describes some experimental results obtained on the conveying of ice particles through the pilot-plant pipeline.

SSDI 0032-5910(95)03026-6

1.1. The nature of the ice particles

Several types of ice makers are commercially available that are suitable for incorporation into large installations through replication of the basic modular units. These units make ice on freezing surfaces in the forms of drums, plates or tubes; the ice forms as a layer with a thickness ranging from a few millimetres to over a centimetre, depending on the design of the machine [2]. In plate or tube machines the ice is harvested periodically by means of a defrosting process in which hot refrigerant is circulated inside the freezing elements. Ice falls from the freezing surfaces and shatters on grids underneath, or is broken up by means of rotating cutters or breaker bars. This ice is in the form of irregularly shaped fragments with a wide distribution of sizes, typically up to 50 mm. In drum machines, thin subcooled flakes of ice are dislodged continuously from the freezing surface by mechanical scrapers. The ice that would potentially need to be conveyed in future mine installations could therefore assume a variety of shapes and sizes. (A further possible form of ice for this application is slurry ice [4], which may also be conveyed pneumatically but is not covered specifically in the present paper.) Two different types of ice machines were used in the experimental programme, described below.

A certain amount of melting of the ice would occur during the transit of the particles through the pipeline, unless the conveying air were to be supplied at an initial temperature well below 0 °C (which would not be economically justifiable). The energy balance for an ice-conveying pipeline has been discussed elsewhere [5]. Melting occurs partly by the conversion, in vertical sections, from potential to thermal energy in the flowing media via friction and impact and partly because of heat transfer through the pipe wall. (The initial cooling of the conveying air has a very small effect.) During a vertical descent of 3000 m through a normally insulated pipeline, for example, 10% of ice initially at 0 °C would be expected to melt due to the energy conversion and a further 5% due to heat transfer. The resulting wetness of the particles was expected to have significant effects upon both the frictional characteristics between the particles and the pipe wall, and the tendency for the particles to agglomerate. A further consequence of conveying melting ice is that the process may be regarded as isothermal, when considering the effects of the compressibility of the conveying air.

In 1850 Faraday described the phenomenon that if two pieces of ice are brought into slight contact in air or water they unite, even when the surrounding temperature is such as to keep them in a thawing state [6,7]. The term 'regelation' was applied to this effect, the explanation for which was the subject of a great deal of unresolved controversy between eminent scientists of the day. Faraday suggested that a 'liquid-like' layer exists on the surface of apparently solid ice and this idea has been revived in recent years to explain many unusual surface properties of ice. It is now generally accepted that a quasi-liquid layer, a few nanometres thick, plays the predominant role in the adhesion of ice and in the sliding friction between ice and a counterface [8,9].

While any wet particulate material will exhibit a certain tendency to agglomerate, the cohesion forces between ice particles are considerably greater [6] than those attributable to the liquid bridges between ordinary wet particles alone [10]. Hobbs [7] postulates that an initial neck forms when two ice particles come into contact, possibly because of local solidification of the liquid-like layer as suggested by Faraday (who reported an intensified effect if a water film was present). The area of the bond would then increase with time through a sintering process, controlled by molecular diffusion through the vapour phase. This qualitative explanation is accepted here as the reason for the pronounced tendency for clustering of ice particles that was observed throughout the pneumatic conveying system from the initial storage point onwards. In particular, this helps to explain the cohesive nature of the ice plugs observed in the underground sections of the conveying pipeline.

The question of the resistance to motion of wet ice sliding along solid surfaces also arises with, for example, plug flow (which occurred in sections of the pilot pipeline). The literature does not give a conclusive explanation of the governing mechanisms but Bowden [11] and Hobbs [7] suggest that since a water film would play an important lubricating role, the angle of contact between water and the counterface material might be related to the coefficient of friction. Bowden showed that hydrophobic surfaces (high contact angle) such as PTFE and uPVC exhibited very low sliding friction coefficients, typically 0.02, while materials that are completely wettable by water (zero contact angle) such as aluminium and steel have much higher friction on snow or ice. The surface roughness of the counterface material may also be important, particularly in the interaction of surface asperities with the proposed quasi-liquid layer [8,9].

To obtain values for the coefficient of sliding friction of wet ice in this project, a series of laboratory tests was carried out using an inclined pipe arrangement. Using wet ice particles of various sizes and in various clusters, with sections of both uPVC and carbon steel pipe, values of 0.020 (st. dev. 0.005) for uPVC and 0.95 (st. dev. 0.32) for steel were obtained. In view of the enormous difference between these values, it seemed very likely that the pipe material chosen would influence the conveyability of the ice, as was confirmed during the conveying tests.

2. Experimental installation

The pilot ice-conveying installation was constructed at East Rand Proprietary Mines Limited (ERPM), the mine that had first suggested the use of ice for underground cooling [12]. The pipeline route is shown diagrammatically in the vertical plane in Fig. 1. The three horizontal sections each also included several bends. As indicated, the flow could be directed in either of two ways on each of the two underground

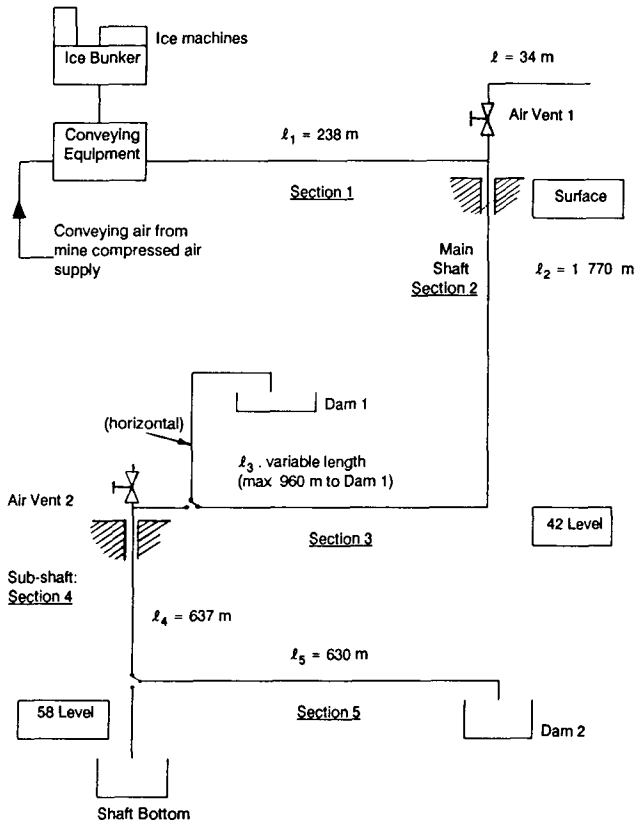

Fig. 1. Pilot installation for underground conveying of ice.

levels, designated 42 level (depth 1770 m below the surface) and 58 level (depth 2407 m), respectively, to provide test pipelines of various configurations. Most of the experimental results given in this paper were obtained with the particular configuration shown in Fig. 2, which also shows the instrumentation employed.

The ice manufacturing plant included a refrigerated storage bunker that could hold some 60 tons of ice (sufficient for conveying test durations of 2 h or more), two ice machines of different types mounted on top of the bunker, and the associated refrigeration plant. The ice machine used in most of the conveying tests operated on a defrosting cycle, producing hollow cylindrical tubes of ice of 34 mm outside diameter and 8 mm average wall thickness, cut into lengths of approximately 30 mm by a rotating cutter. The second machine produced 3 mm thick ice flakes, typically 20 mm across, dislodged continuously from the freezing surface (the inner surface of a circular drum) by means of a rotating scraper. Ice was delivered out of the storage bunker by means of a variable-speed screw conveyor.

Two types of pipeline feeding devices were used, namely, blow vessels and a rotary valve. The mixed experience with the blow vessels has been described elsewhere [3]; all the results given here were obtained using the rotary valve, which proved more suitable. This was a conventional commercially available valve of the unvented blow-through type (blowing seal), with a ten-vane 450 mm diameter stainless-steel rotor, fitted with a variable-speed drive. Careful tests were carried out to measure the air leakage and feed rate characteristics of the valve [5], the latter particularly because it was used as a calibrated feeder to measure the ice flow rate during the underground conveying tests. (The results of the calibration tests were generally consistent with air leakage and feed rate characteristics for drop-through rotary valves, reported previously by Reed and Kessel [13] and Reed and Mason [14] respectively.) Conveying air was drawn via a pressure reducer from a large compressed air main, as indicated in Fig. 2.

Underground conveying tests were first carried out using an insulated steel pipeline, with an inner diameter of 97 mm. Some encouraging results were obtained; in particular, no blockages were experienced at the bend at the lower end of the vertical pipeline. However, the reliability of conveying

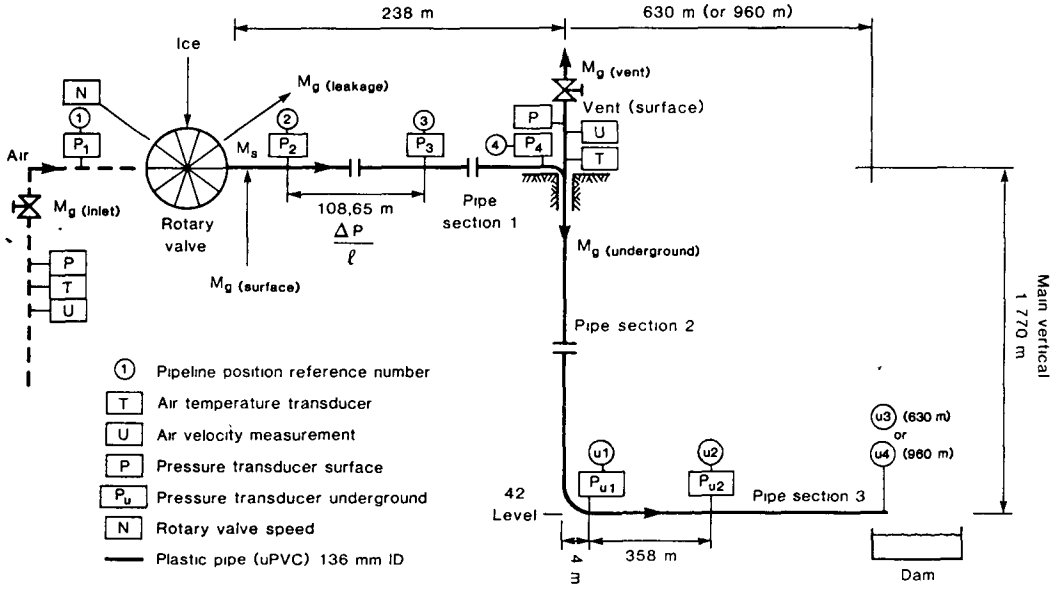

Fig. 2. Pipeline configuration and instrumentation for conveying tests to 42 level of the mine.

was otherwise poor, with frequent blockages occurring at the upper end of the vertical section. The blockages were due to particle bridging, influenced by the ice type and condition (wetness and particle size distribution) and by the ice and air flow rates. As already mentioned, wet ice is highly cohesive and adhesive to steel surfaces and this explains the blockages. In the light of these results an all-plastic pipeline was installed for further testing, using non-insulated uPVC piping with an inner diameter of 136 mm and 12 mm wall thickness. To allow thermal contraction in the pipeline down the mine shaft, 194 sliding joints were provided along this section, with one at the end of each 9.1 m length of pipe. An air release connection with a shut-off valve was provided at the top of the vertical section, so that the effect of venting some conveying air could be determined.

Using the instrumentation shown in Fig. 2, a continuous record of ice and air mass flow rates through each section of the pipeline was obtained throughout each conveying test. Static pressure was also recorded at four points along the surface section of the pipeline and two points along the underground section. It was not feasible to install any measuring devices along the vertical section in the mine shaft. A few high-speed films were taken underground through transparent pipe sections close to positions u1 and u2 (Fig. 2), as well as flash photography at the discharge point, to show the nature of the flow. High-speed photography was also used to record the nature of the flow through the surface pipeline.

3. Experimental results — general

The experimental results described here are primarily those obtained during the underground conveying tests through the 136 mm bore uPVC pipeline shown in Fig. 2. More than 120 tests were carried out using this pipeline configuration, the main variables being the ice flow rate, the air flow rate and the status of the air vent valve (open or closed). Two important general findings from these tests were:

- no blockages at all were experienced in the below-surface sections of the pipeline, confirming that there was a great difference between carbon steel and uPVC piping regarding the conveyability of ice;
- there were no discernible differences in conveying performance between flake ice and tube ice.

The ice flow rate during these tests reached a maximum value of 7.4 kg/s, limited only by the capacity of the equipment for feeding ice into the pipeline.

Twenty further tests were also carried out with the pipeline extended down the subshaft to 58 level (Fig. 1). Trouble-free conveying was sustained on several occasions, with ice flow rates of up to 6.3 kg/s for a maximum total length of the pipeline of 3905 m (to Dam 2, Fig. 1). Blockages were, however, experienced in the second vertical section (section 4) of the pipeline during some tests. These were attributed to the jamming of long plugs of ice in the sliding joints installed in this second vertical pipe section. (The absence of blockages at the same sliding joints in the first vertical pipe section may be explained by the different nature of the flow at that stage, being dilute phase.) From a practical point of view it is believed that blockages could be avoided in future by installing a different type of joint, not having any irregularities in the pipe bore. With this proviso, this phase of the experimental programme was also judged to be successful.

The nature of the flow through the various sections of the pipeline is next described, with particular reference to the 'tube' ice, before details of the experimental results are discussed.

4. The nature of the flow through the various sections

4.1. Pipe section 1: horizontal pipeline on the surface

High-speed photography through transparent pipes showed the nature of the flow through the horizontal pipeline attached to the rotary valve. The flow patterns observed were essentially the same as those described in the literature for horizontal pneumatic conveying of various materials. Wen and Simons [15], Richardson and McLeman [16], Owen [17], Konrad [18], Molerus [19] and Tsuji and Morikawa [20], among others, have described the main flow features that become prominent as the conveying air velocity is reduced. In the present investigation the ice particles were unusually large in relation to the pipe diameter, with d/D up to 0.35. Nearly all publications have described work in which d/D is much less than 0.1. Nevertheless, the same salient ice flow characteristics were readily recognizable.

With high air velocities in pipe section 1, above 40 m/s at a given point, the ice particles moved in fully suspended dilute-phase flow and were uniformly distributed over the cross section of the pipe, with little noticeable bouncing against the walls. At lower velocities of 30 to 40 m/s there was a pronounced tendency for most of the particles to travel smoothly in suspension in the lower portion of the pipe, with isolated small particles above. This is described by Konrad [18] as 'stratified' as distinct from 'fully suspended' dilute-phase flow. As the air velocity was reduced below 30 m/s, the particles started to settle and form clusters sliding along the bottom of the pipe. Clustering is mentioned by Owen [17] as a characteristic of flow near the 'saltation point'. With relatively high values of the ice/air mass flow ratio μ (more than 10) these clusters became quite long (about 1 m).

At an air velocity of approximately 27 m/s the signal from a pressure transducer mounted in the pipeline started to include significant fluctuations, showing that occasional clusters filled the entire cross section of the pipe as plugs. (This plug formation occurred first in downstream proximity to bends but the typical velocity values mentioned here refer to a position at the end of a long straight length of pipe after a bend.) A further reduction in air velocity resulted in a flow of nearly full-bore plugs spaced at regular intervals. With

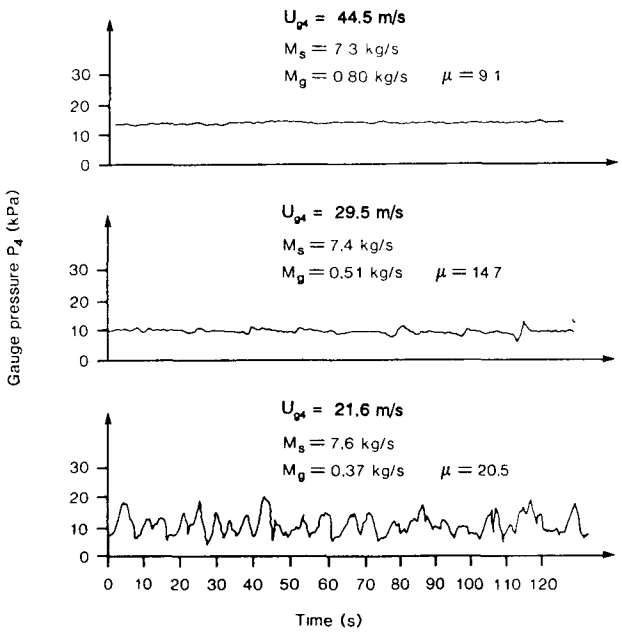

Fig. 3. Pressure–time traces showing initiation of plug flow as air velocity is reduced.

other more common particle/pipe material combinations, blockages would generally be expected to occur shortly after the commencement of saltation (i.e. at approximately 30 m/s here). In this case the very low friction between wet ice and plastic permitted stable plug conveying to continue until the air velocity was reduced below approximately 20 m/s, after which blockages occurred.

These typical flow characteristics are illustrated in Fig. 3 for three particular tests carried out with progressively lower air velocities, the ice flow rate being kept constant (apart from the normal flow fluctuations experienced with a rotary valve feeder). This figure shows pressure–time traces taken at position '4' (Fig. 2). In the last test, at a superficial air velocity of 21.6 m/s at that point, the pronounced and regular fluctuations indicate the passage of full plugs.

These flow pattern observations essentially correspond to those described by Molerus [19], although his descriptions were written with smaller particles in mind, the largest being 8 mm beans conveyed in a 50 mm pipe. The necessity to make a distinction between large and small particle flow patterns is emphasized by Boothroyd [21] and Tsuji and Morikawa [20]. The latter state that with small particles the formation of long plugs causes blockages, but that stable plug flow is possible for large particles if the solids flow rate is not too high.

Fig. 4 shows a typical set of conveying results for pipe section 1 in the format of the well-known 'phase diagram' or 'state diagram' [22]. The pressure gradient was measured along a 108.65 m length of straight pipe and the superficial air velocity is the mean value within that length. All the points in this figure represent 'dense-phase' flow, using this term to encompass all forms of flow where the gas velocity is insufficient to support all the particles in suspension. Blockages (dotted line) appeared to occur at a particular air mass velocity, corresponding to a decreasing air velocity as the ice flow rate increased. Further observations on the conditions causing blockages are discussed in a later paragraph.

4.2. *Pipe section 2: vertical pipeline in mine shaft*

It was not possible to make direct observations of the flow within the vertical pipeline in the mine shaft. The nature of the flow down this pipe column had therefore to be deduced from pressure measurements and visual observations made at the upper and lower ends.

During these conveying tests full plug flow in pipe section 1 on the surface was avoided. The flow entering the top of the 1770 m vertical section was consequently characterized by steady pressure recordings with no significant fluctuations. Pressure was also monitored at the lower extremity of the section, normally just after the bottom bend (position u1, Fig. 2). This pressure record was also steady during all the conveying tests. No fluctuations were observed that would have indicated the existence of plugs at the lower end of the vertical section. Ice plugs did form shortly after the bottom bend, as described below, with very distinctive changes to the flow characteristics. Since there is no reason to believe that plugging might have taken place during the descent of the ice, it may be concluded that the flow was of the dilute-phase type. This was the case irrespective of whether the air vent valve at the top of the section was open or closed. (When open, air was normally expelled from this vent, except during tests with low values of air flow rate in pipe section 1, when air was sucked in through the vent.) The degree to which ice clusters disintegrated or formed during the descent remains a matter of speculation.

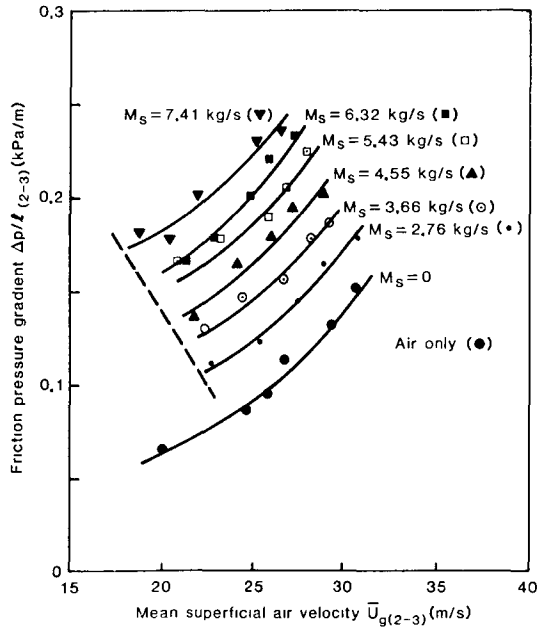

Fig. 4. Typical phase-diagram plot of surface pipeline pressure gradient measurements.

Fig. 5. Full ice plugs emerging on 42 level at an ice flow rate of 2.76 kg/s.

A factor that could also come into consideration is the difference in falling velocities of particles of various sizes, but this would not seem likely to change the pattern of the flow. By the time that the ice reached the bottom of the vertical section the particles were fairly uniform in size (about 10 to 15 mm) with most of the initial tubes having shattered and most of the fines having melted. This was observed by opening the pipeline immediately after the bottom bend and sampling the ice. During these observations there was no indication of cohesive plugs; the only nonuniformity in the ice flow was a small fluctuation attributable to the feeding action of the rotary valve.

4.3. Pipe section 3: horizontal pipeline underground

The ice flowed along the horizontal pipe section 3 on 42 level of the mine in the form of plugs or slugs in all the tests. The terminology 'plugs' or 'slugs' is used here for ice particles more, or less, tightly packed in the pipe, respectively. The nature of the flow that emerged from the end of this pipeline (see Fig. 5) was essentially the same irrespective of the length of section 3 (between 30 and 960 m), the number of bends within this section (up to six sharp bends), or the opening or closing of the air vent valve on the surface.

The formation and flow of the ice plugs were first studied by taking pressure records at various points along the pipe. Significant fluctuations, particularly at low ice flow rates (see Fig. 6(a)), were detected along the entire 42 level pipeline after a position typically 20 m downstream of the vertical-plane bend located at the bottom of the vertical section. A very noticeable low-frequency sound also emanated from the pipe at this position. High-speed photography through a transparent section at this point revealed the mechanism of plug formation clearly.

Following their impact against the pipe wall in the bend at the bottom of the vertical, the ice particles emerged into the horizontal section as clusters, sliding slowly along the bottom of the pipe. At this point the clusters usually filled less than half of the cross section of the pipe and varied in length, depending on the ice flow rate, from 0.2 to 2 m. Successive clusters were separated by much longer air spaces; this separation into distinctive clusters may perhaps have originated from the periodic feeding characteristic of the rotary valve. Because of the low air velocity due to air compression down the vertical section (discussed later) there was no possibility of re-entrainment of ice particles into the air flow. Since the air could generally flow freely above the clusters, few large pressure fluctuations were detected near the bend (see the pressure trace P_{u1} in Fig. 6(a)).

After emerging from the bend into the horizontal section, some clusters would come to a standstill about 20 to 50 m downstream, particularly at low ice flow rates. A following cluster having a greater momentum would then collide with any stationary or slower-moving cluster; during the impact the ice could be forced into a full-bore plug that would either be set into sliding motion along the pipe or would remain stationary until the next collision, depending upon the momentum of the incident cluster.

Fig. 7(a) is a frame from a high-speed film taken 50 m from the bend, showing a stationary cluster on the right and a following cluster sliding towards it from the left. Neither cluster occupies the full cross section of the pipe at this instant. Fig. 7(b), at a short time later, shows that just after the collision the ice is being compacted into a full-bore plug on the right. The ice on the left is still moving into this plug, which is being accelerated into motion. The result of this shunting process was the formation, at the lower ice flow rates, of a succession of widely separated plugs that moved steadily through section 3. Fig. 7(c) shows an unusually short plug, with typical shapes of the leading end (on the right) and bluff trailing end, moving through the pipe at a position 600 m from the bend. At this location few collisions were observed, although differences in measured velocities of individual plugs (between 1 and 4 m/s) implied that some col-

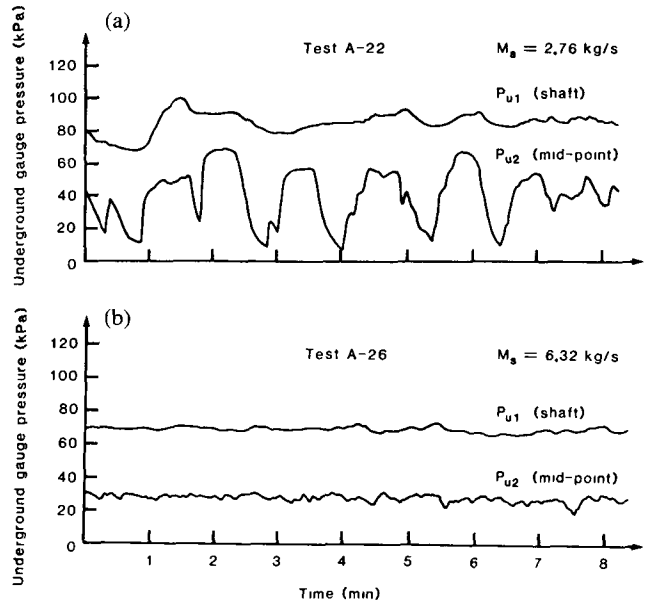

Fig. 6. Pressure–time traces at positions u1 and u2 on 42 level, at ice flow rates of (a) 2.76 and (b) 6.32 kg/s.

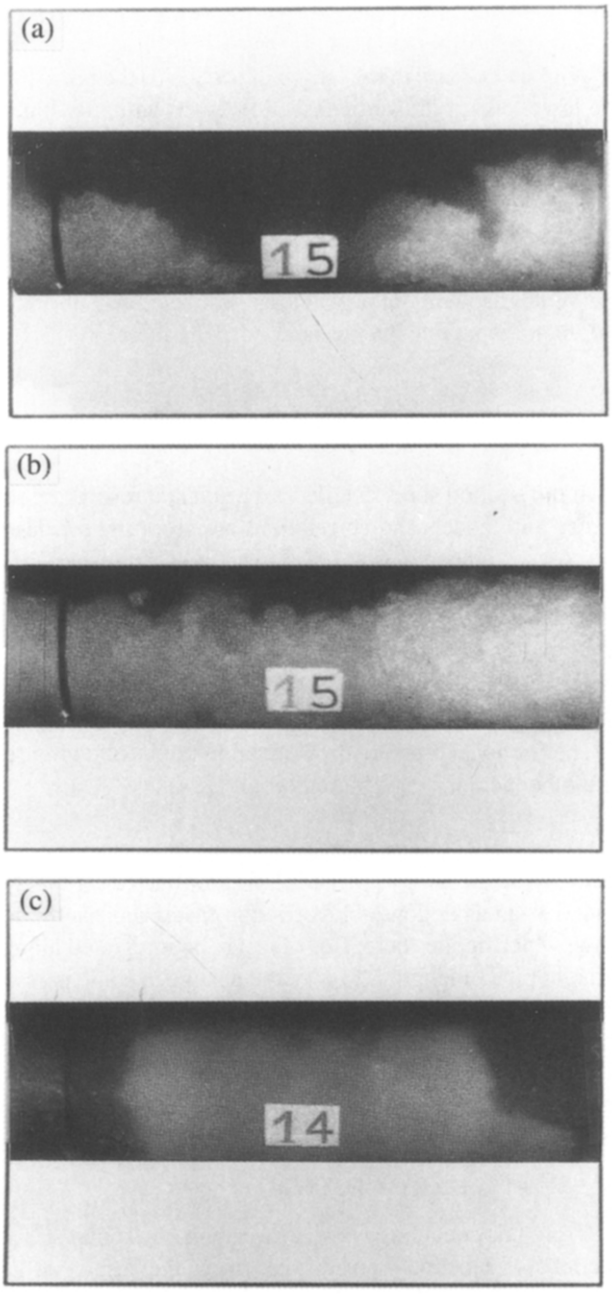

Fig. 7. Frames from high-speed film of the formation and passage of ice plugs on 42 level (flow from left to right): (a) plug formation 50 m downstream of vertical bend into pipe section 3; ice flow rate 4.55 kg/s, air flow rate 0.71 kg/s; (b) the same position a very short time later; (c) passage of a short plug 600 m downstream of the vertical bend; ice flow rate 2.76 kg/s, air flow rate 0.72 kg/s.

lisions would occur along the pipeline from time to time. The pressure trace P_{u2} in Fig. 6(a), at an ice flow rate of 2.76 kg/s, indicates a fairly regular succession of plugs moving past a position 360 m from the bend at a rate of approximately one per minute.

At higher ice flow rates the nature of the flow changed. Instead of a succession of widely spaced tight-fitting plugs there was a more continuous flow of long slugs that did not quite occupy the full bore. Under these conditions the pressure traces from both underground transducers, particularly from the midpoint (P_{u2}), were steadier. Fig. 6(b) shows a typical pair of traces at an ice flow rate of 6.32 kg/s. Fig. 8 shows an ice slug at the end of the pipeline at a flow rate of 4.55 kg/s and evidently it had not filled the cross section of the pipe. It seems that with a more continuous ice flow at the higher rates there was less likelihood of ice coming to a standstill on emerging from the vertical section and then being impacted from the rear.

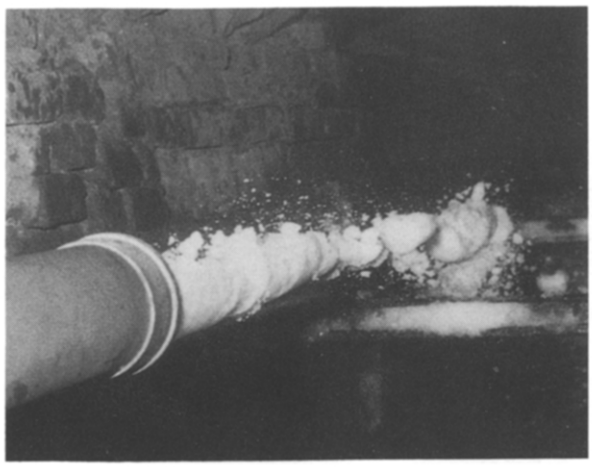

Fig. 8. Loose ice slug emerging on 42 level.

This change from plug flow to slug flow occurred at an ice flow rate of approximately 3 kg/s in all the tests with an open air vent at the upper end of the vertical column. When the air vent was closed and greater quantities of air were consequently forced through the underground pipeline, the transition occurred within the range of flow rates from 4 to 6 kg/s, depending upon the respective air flow rates. In each case this flow transition was accompanied by a reduced total pressure loss along section 3 (see Fig. 16).

4.4. Pipe sections 4 and 5 down subshaft system

In the tests carried out through the pipeline after it was extended down the subshaft, the ice entered the vertical section 4 as long slugs (or shorter plugs) as described above. Once in the vertical pipe the ice re-formed into long wet plugs that filled the pipe. As mentioned already the blockages experienced in section 4 were attributed to these plugs jamming at the irregularities in the pipeline, particularly in the expansion joints.

5. Overall aspects of the flow through the pipeline

Fig. 9 illustrates the salient characteristics of the flow through the complete pipeline. It includes static pressure and superficial air velocity profiles for three pipeline configurations, covering two lengths for section 3 and two states of the air vent (open or closed) at the top of the vertical section. The ice flow rate (7.4 kg/s) and the air flow rate (0.7 kg/s)

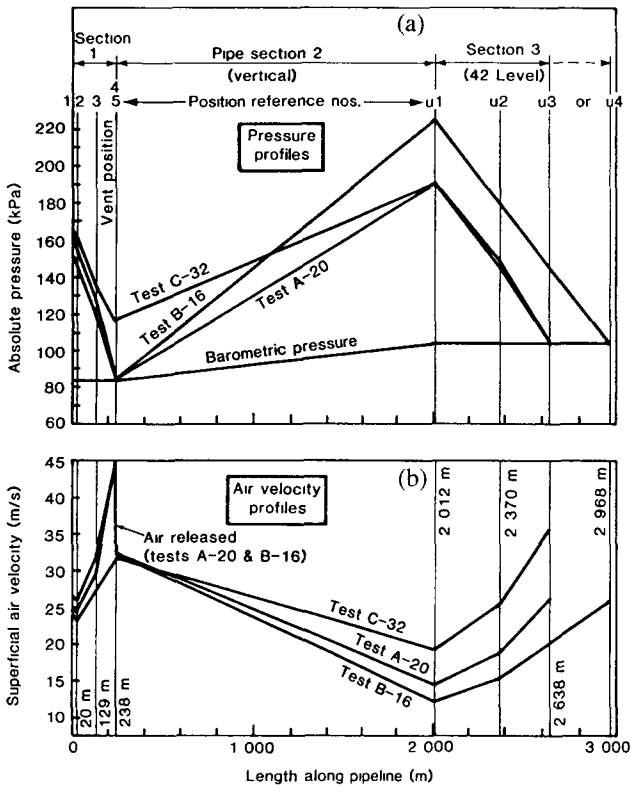

Fig. 9. Static pressure and air velocity profiles along complete pipelines of three different configurations to 42 level, for the same initial ice and air flow rates. For each test: ice flow rate 7.4 kg/s; air flow rate in section 1 is 0.7 kg/s; pipe ID 136 mm. Pipeline configurations: test A-20: vent open, length of section 3 is 630 m; test B-16: vent open, length of section 3 is 960 m; test C-32: vent closed, section length of 3 is 630 m.

were the same in each of these tests. Up to 20% of the ice, entering at 0 °C, melted in transit through the pipeline in each of these tests [5]. The measured points are joined by straight lines in Fig. 9 to reflect average pressure gradients in the respective pipe sections (the actual profiles are considered later). In the two open-vent tests 28% of the initial conveying air escaped to atmosphere at the end of section 1 and so the air flow rates underground were different from that in the closed-vent test. The following observations may be made:

- The air velocity first decreased within the acceleration zone after the rotary valve because the conveying air was being cooled by the ice. After that there was a large velocity increase along section 1, particularly with the vent open. Clearly any pressure loss models need to take the air compressibility into account — this is true throughout the pipeline.
- In all cases there was a large rise in gauge pressure and a corresponding decrease in air velocity down the length of the vertical column. The superficial air velocity at the foot of the column was generally less than 15 m/s for the open-vent tests and less than 20 m/s for the closed-vent tests. These velocities were below that resulting in plug formation in even a straight pipe, as observed in pipe section 1. It is therefore clear that a transition from dilute phase to plug flow would occur at the start of section 3. Marjanovic et al. [23] observed the same flow characteristics at the bottom of a vertical pipe in a laboratory-scale system.
- With an increase in the length of section 3, the pressure at the lower end of the vertical section 2 was naturally higher. The vertical pipeline may be regarded as a self-regulating air compressor, in the sense that it generated the pressure required to propel ice along the subsequent horizontal pipeline. The system would eventually block if the length of section 3 became so great that the pressure rise generated in the vertical column, at a given ice flow rate, was no longer sufficient to provide the necessary driving force.

6. Experimental results for the respective sections

In this section some detailed experimental results are presented and models and correlations are proposed for design purposes. Comparisons are also made with published information.

6.1. Horizontal flow through pipe section 1

(i) Conveying line pressure drop

The frictional pressure drop equation used, following several other authors, e.g., Marcus et al. [22], is:

$$dp_f = dp_g + dp_s = (\lambda_g + \mu\lambda_s)\rho_g U_g^2 dL/2D \quad (1)$$

where λ_g is the Darcy–Weisbach friction factor for air flow and λ_s is an analogous solids friction factor. For isothermal flow, which applies here, Eq. (1) may be integrated along a straight pipe of length L to give the change in static pressure from a position '1' to a position '2', taking air compressibility into account. (The conventional assumptions made in doing so are that λ_s is approximately constant over this distance and that the acceleration pressure drop associated with the air expansion may be neglected.) The result is:

$$p_1^2 - p_2^2 = (\lambda_g + \mu\lambda_s) M_g^2 RTL/DA^2 \quad (2)$$

Using this equation, values of λ_s along horizontal straight sections of pipeline were derived from the results of 258 conveying tests with 136 mm bore pipe and 34 supplementary tests with 95 mm bore pipe, also of uPVC. A planned investigation into the effects of using other pipe diameters could unfortunately not be taken further than this, for practical reasons.

A representative selection of the results is shown in Fig. 10 to illustrate the salient features observed. In these particular series of tests, carried out on the surface, the flow was characterized as either dilute phase or dense phase based on both the degree of unevenness of the pressure records (see, e.g., Fig. 3) and the appearance of the flow at the pipe outlet. In Fig. 10 the solid symbols represent dense-phase flow and the open symbols represent dilute-phase flow. At the transition between the two, at a Froude number (Fr) of approximately 600 (corresponding to a mean test section air velocity U_g of approximately 27 m/s in a 136 mm pipe and the first

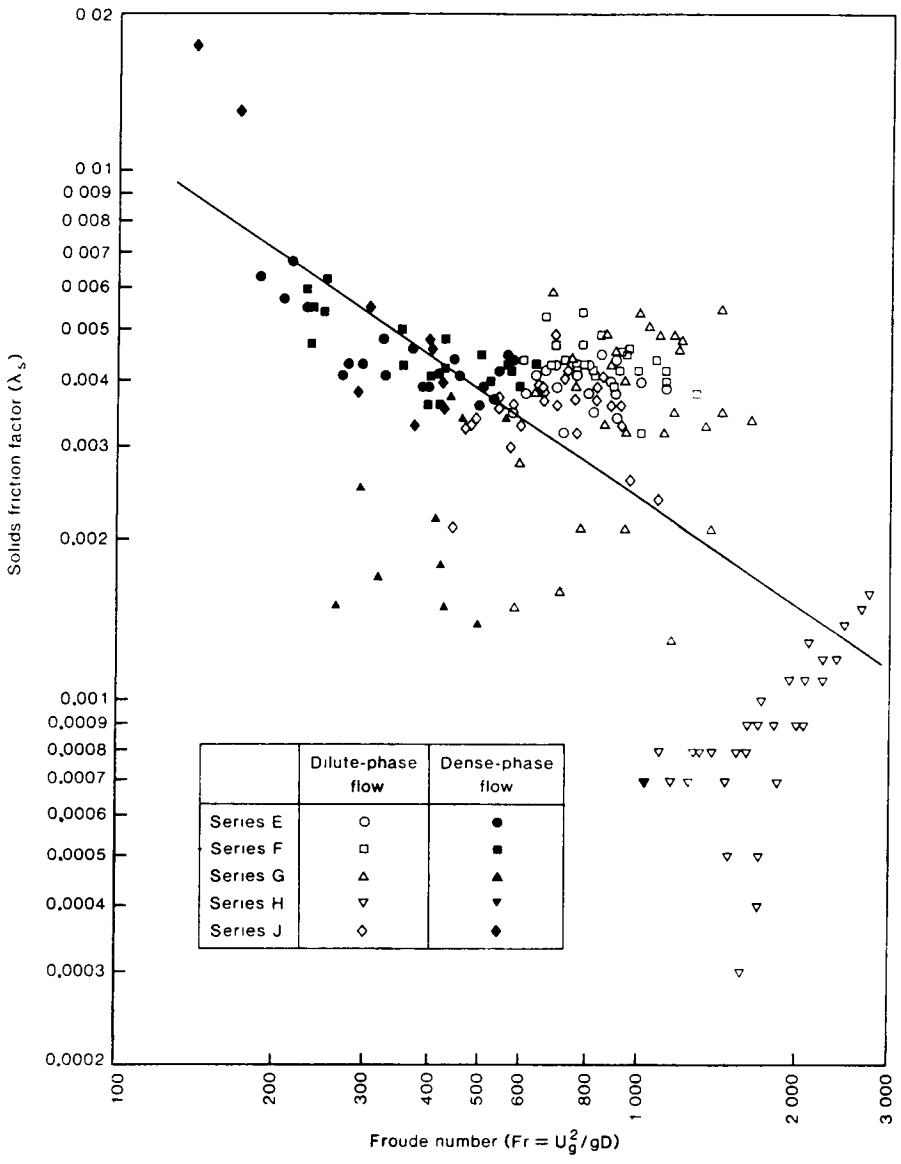

Fig. 10. Solids friction factors for horizontal pipes plotted against Froude number.

appearance of plug flow), it appears that there might well be a change in the relationship between λ_s and Fr. It is also observed that the λ_s values for the 95 mm pipe (test series H) are significantly lower; it seems that the pipe diameter (presumably in the form d/D) has by far the greatest influence on the solids friction factor. Although they would be more appropriate, multifactorial correlations such as $\lambda_s = \lambda_s(Fr,\mu,d/D)$, for the two regions of flow separately, cannot justifiably be proposed here, since only two values of D were tested. Instead, a simple correlation for design purposes was found, covering the whole Fr range in the tests:

$$\lambda_s = 0.084 Fr^{-0.5} \quad (n = 292,\ r^2 = 0.27) \tag{3}$$

Several published correlations applicable to 'coarse' materials were compared with the λ_s test results for ice. Michaelides and Roy [24] derived a correlation identical to Eq. (3), except for the value of the coefficient, by analysing a large base of data from various publications for ten coarse materials flowing through steel pipes. They recommended a coefficient of 0.076 as a 'middle of the road' value for all these substances. Equally close general correspondence to the measured values was obtained by using a more detailed correlation by Hitchcock and Jones [25], which does feature a dependence of λ_s on the d/D ratio. Of other correlations, that by Hinkle [26] gave quite close values for the smaller pipe but seemed less suitable for larger diameters, while the same applied to that by Rose and Duckworth [27], which was generally less accurate. Correlations by Weber [28], Barth [29] and Scott [30] gave completely incorrect answers.

Some published correlations for the solids friction factor λ_s require a knowledge of the solids/gas velocity ratio U_s/U_g. Values of this ratio for ice particles were obtained by high-speed photography for various air velocities and particle sizes, and for three pipe diameters. Fig. 11 shows some results

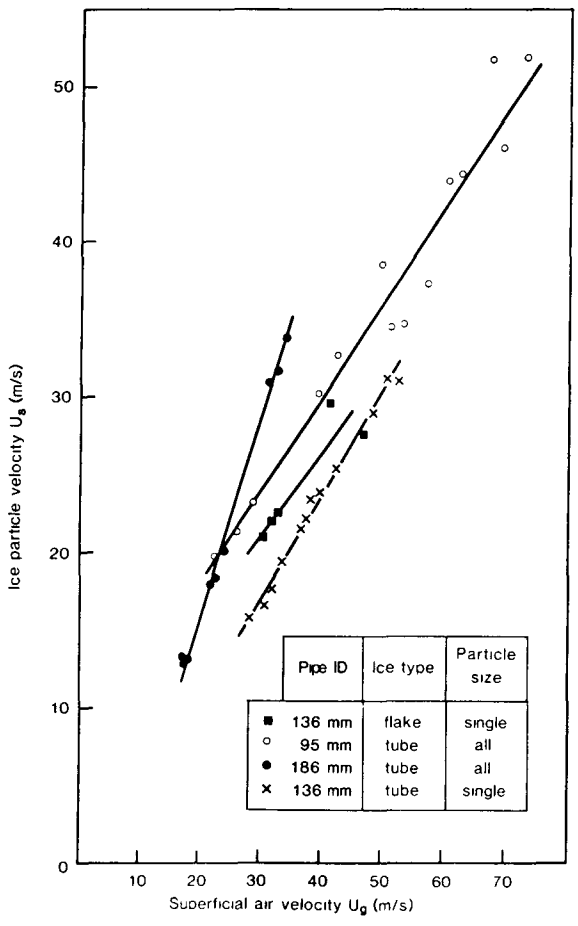

Fig. 11. Relationships between ice particle velocity and air velocity for various pipe diameters and ice types, for horizontal flow.

for the various pipe diameters and ice types. With a 95 mm bore pipe the ice particles were distributed uniformly in dilute-phase flow throughout the air velocity range. The particle size, whether of tube ice or flake ice, was not a significant factor. In the 136 mm pipe the flow was stratified dilute phase; the particle size influenced the velocity ratio, although not to the same extent as did the pipe diameter. The particle size effect is illustrated in Fig. 11 by the comparison between single ice tubes (34 mm diameter) and single flakes (thin flakes 20 mm across) for a 136 mm diameter pipe. A good average value of U_s/U_g for this pipe was 0.6, with values of up to 0.7 for small particles of a few millimetres. With the 186 mm pipe there was a change in the type of flow from pronounced stratified flow at the higher velocities to sliding flow at the lower velocities, but this did not change the slope of the line in Fig. 11. No particle size influence was detected.

The measured velocity ratio data were compared with four (widely differing) published correlations for coarse particles. None of these matched the measurements adequately. The closest correspondence was given by the expression by Richardson and McLeman [16], followed by those of Hitchcock and Jones [25] and Klinzing et al. [31]. The expression by Rose and Duckworth [27] gave the worst correspondence, with predictions typically of half the measured values. A correlation for ice particles is not proposed here; a more extensive data bank would clearly be a pre-requisite.

During 29 of the conveying tests through the 136 mm bore pipe, the total pressure loss Δp_b across a 90° horizontal bend of radius 0.57 m was measured. This Δp_b was defined in the same way as by Morikawa et al. [32] and included the downstream acceleration loss. The total bend pressure loss Δp_b, expressed as a multiple of the pressure loss across the same length of straight pipe, appeared to increase linearly from approximately 10 at $Fr=600$ ($U_g=28$ m/s) to 30 at $Fr=1200$ ($U_g=40$ m/s). The pressure loss ratio due to the solids alone was derived by deducting the air-only bend pressure drop, calculated by the generally accepted correlation by Ito [33], from the total Δp_b. This ratio increased from approximately 10 at $Fr=600$ to 50 at $Fr=1200$.

These results were compared with the prediction from the Schuchart equation [34]. Schuchart found that the solids pressure loss ratio depended only upon the bend diameter/pipe diameter ratio, with his correlation giving a value of 18 for the bend used here. The results were also compared with the bend loss coefficient recommended by the Engineering Equipment Users' Association (EEUA) [35]. Their relatively simple approach, depending again only upon the bend diameter ratio, was also found to give a reasonable estimate for practical design purposes at normal conveying velocities, although again the clear Froude number dependency found for ice particles is not catered for in this method.

(ii) Minimum conveying air velocity

Some supplementary tests were carried out in an attempt to determine the factors associated with flow regime transition, particularly with respect to incipient blockage conditions. Three short pipelines were used ($D=95$, 136 and 186 mm), all following similar routes incorporating two 90° bends.

One common definition of the boundary between the dilute-phase and dense-phase regions is given by the 'pressure-minimum' velocity, found by plotting a phase diagram. Another definition is the saltation velocity, being the velocity at which the largest particles are no longer suspended in the flow but fall out and slide along the bottom of the pipe. A further point of transition identified by Wirth and Molerus [36] occurs when sliding-cluster flow changes to full plug flow as the air velocity reduces, with the accompanying onset of marked pressure pulsations. Finally, a critical velocity in the ultimate sense of the minimum air velocity to avoid pipe blockage may be observed. The pressure records taken during the conveying tests on surface, with the high-speed photography and visual flow observations, allowed minimum conveying air velocities at the inlet of the pipeline to be found in terms of these four respective criteria, over the pipe diameter range tested. The results are given, in a condensed form, in Fig. 12.

The pressure-minimum velocity has frequently been used in the literature to define 'saltation' conditions. No sets of saltation data based on photographic evidence seem to have

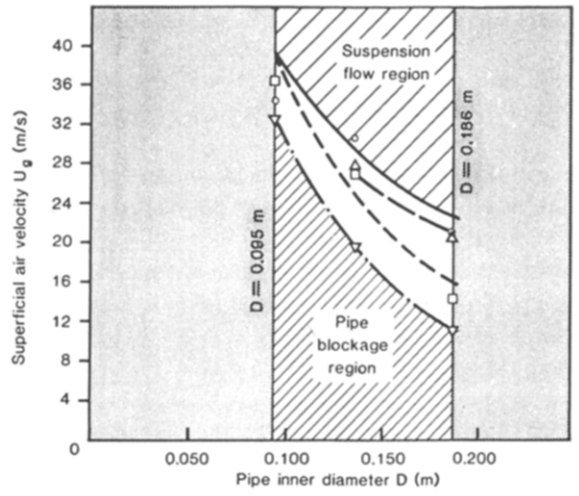

Symbol	Criterion	Fitted line	Coefft of determination
o	Visual saltation	$U_g = 5.69\ D^{-0.82}$	$r^2 = 0.52$ (n = 33)
△	Plug flow	$U_g = 5.43\ D^{-0.80}$	$r^2 = 0.31$ (n = 30)
□	Pressure-minimum point	$U_g = 1.66\ D^{-1.35}$	$r^2 = 0.85$ (n = 29)
▽	Minimum conveying velocity	$U_g = 0.75\ D^{-1.61}$	$r^2 = 1.00$ (n = 3)

Fig. 12. Flow transition observations from suspension flow to blockage in a horizontal pipe, downstream of a pair of bends, as a function of pipe diameter. Note: the symbols each denote the mean values of several points (except for those on the minimum curve), which are not shown here individually.

been published with which a comparison with the ice particle data could be made. It was noteworthy throughout the experimental programme that there was visual evidence of slugging and then of plug flow before the pressure-minimum point was reached, as the air velocity was reduced, as indicated in Fig. 12. The initiation of plug flow was, however, clearly influenced by the presence of the bends in the pipeline and the results obtained would not be comparable with flow transition results from straight pipes. The same applies to initial saltation and to ultimate blockage. The trend of decreasing transition velocities with increasing pipe diameters should therefore be regarded as indicative for practical pipelines incorporating bends.

One noteworthy finding was that the mass flow ratio μ did not appear to have any influence on the transition velocity or minimum conveying velocity, within the range tested of μ up to 20. There was also no discernible difference between the tube ice and flake ice observations. Furthermore, the strong influence of the pipe diameter shown in Fig. 12 could not be catered for by applying any of the published Fr-based correlations [29,36,37], which apply to straight pipes.

While Fig. 12 leaves some fundamental questions unanswered, it may be used as a basis for a practical guideline for ice-conveying pipelines made from uPVC material. The recommendation here is to use the pressure-minimum velocity as the basis for the air supply system design. This would give a margin of approximately 4 m/s above the blockage velocities observed at the same point in the pipeline. In the tests this point was located downstream of two bends arranged close to each other. If this correlation $U_g = 1.66D^{-1.35}$ m/s is conservatively applied at the solids inlet to the pipeline and a generous length of straight pipe (at least $200D$) is provided immediately downstream, before any bend, then trouble-free ice conveying would be assured for pipes within the size range tested. For all larger pipes an inlet air velocity of not less than 14 m/s is recommended. A significant aspect of the adoption of the pressure-minimum correlation as a design guideline is that the flow along at least some parts of the horizontal pipeline will be of a dense-phase nature. Fig. 12 shows that it would not be economical to design for suspension flow of such large particles in a horizontal pipeline.

6.2. *Vertical flow through pipe section 2*

The proposed physical model of dilute-phase flow down a long vertical section is described with reference to Fig. 13. This model applies equally to flow conditions with the air vent valve closed or open. The particles entering the top of the vertical pipe accelerate under gravity, past the position at which the particle velocity is equal to the air velocity, until

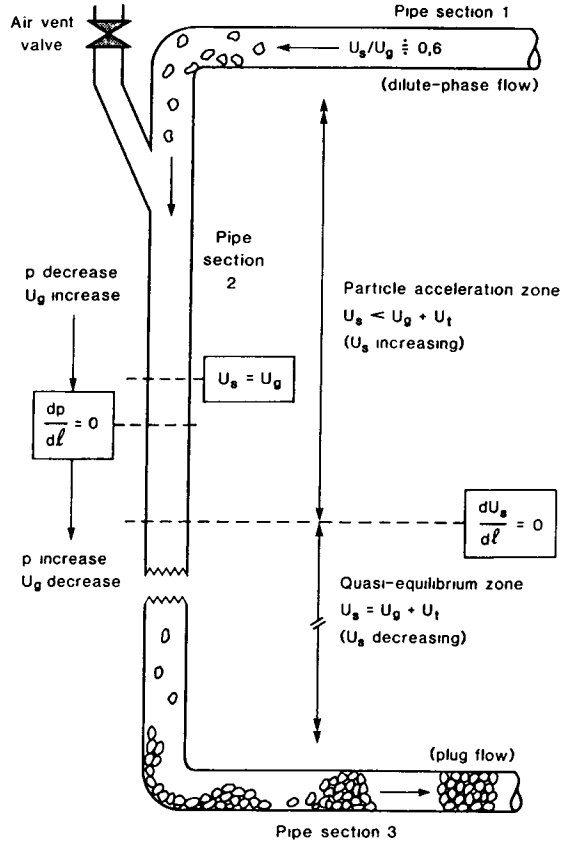

Fig. 13. Regions of downward gas–solids flow in a long vertical pipe column followed by a horizontal pipeline.

the point is reached where the particle velocity exceeds the air velocity by the particle terminal velocity relative to the air. The length of pipe down to this point constitutes the acceleration zone. If the air were incompressible, an 'equilibrium zone' would occupy the remainder of the pipe (McDougall [38], Stinzing [39], De Jong [40]). In the real case the pressure and air density increase substantially down the length of the pipe, commencing shortly after the point at which the particle velocity becomes greater than the air velocity.

The value to which the pressure rises at the foot of the column is determined by the resistance to flow through the succeeding horizontal pipe section; the vertical column is in effect an air compressor that provides an equilibrium pressure sufficient to maintain the downstream horizontal plug flow. The consequence of the pressure rise down the column is a corresponding decrease in air velocity, which in turn causes the particle velocity to reduce to maintain approximately the same terminal velocity relative to the air. In such a long end-restricted vertical column, therefore, the particle acceleration zone is followed by a long and gradual particle deceleration zone, which may be regarded as a quasi-equilibrium zone.

The procedure described below for calculating the solids friction factor λ_s for downward vertical flow, given pressure measurements (and therefore air velocity values) at the upper and lower extremities of the column, incorporates several assumptions that have been examined by Sheer [5]. The first is that the pressure change due to the particle acceleration at the top of the vertical section is negligible in comparison with the overall pressure change in this very long section. The equation for the total change in pressure is then:

$$dp_{tot} = dp_f + dp_z = -(\lambda_g + \mu\lambda_s)\rho_g U_g^2 dL/2D + g[\rho_g \epsilon + \rho_s(1-\epsilon)]dL \quad (4)$$

where dp_{tot} is the increase in pressure along a vertical length dL, L being taken as positive in the downward direction. The quantities ρ_g, U_g (and therefore presumably λ, where $\lambda = \lambda_g + \mu\lambda_s$) and the voidage ϵ ($\epsilon = 1 - M_s/\rho_s U_s A$) vary with L. (One point at which ϵ may be calculated is where $U_s = U_g$, Fig. 13; a typical value was 0.98.) By making the simplification that $\rho_g \epsilon \approx \rho_g$, Eq. (4) may be written:

$$\frac{dp_{tot}}{dL} = -\lambda\frac{RTM_g^2}{2DA^2p} + \frac{gp}{RT}\left(1 + \mu\frac{U_g}{U_s}\right) \quad (5)$$

To find experimental values for λ, some assumption had to be made regarding the behaviour of U_s before Eq. (5) could be integrated. The assumption chosen was that, for any particular test, U_g/U_s could be regarded as approximately constant [5]. Assuming again (as for pipe section 1) that λ_s is approximately constant along the whole length of the vertical section during a particular test, the integration gives a value for λ as a function of the measured pressures:

$$\frac{p_2^2 - \lambda a/(1+\mu U_g/U_s)}{p_1^2 - \lambda a/(1+\mu U_g/U_s)} = \exp[2gL(1+\mu U_g/U_s)/RT] \quad (6)$$

where p_2 = absolute pressure at foot of column, p_1 = absolute pressure at top of column, $\lambda = \lambda_g + \mu\lambda_s$ and $a = R^2T^2M_g^2/2gDA^2$ (constant during a test).

For a mass flow ratio $\mu = 0$, this equation reduces to that for air flow alone and this allowed values of λ_g to be obtained for various values of M_g, and thence values of λ_s for corresponding two-phase flow tests.

An average value of U_g/U_s for each test, taking U_g to be the mean of the inlet and outlet air velocities, was calculated for an average-sized particle (equivalent spherical diameter 18 mm) by using published information. This involved calculating the terminal velocity for a falling particle, using a drag coefficient based upon values for non-spherical particles proposed by Haider and Levenspiel [41]. Corrections were introduced in an attempt to take into account particle–particle and particle–wall interactions, using techniques similar to those proposed by Yang [42] but modified for downward flow. The values of U_g/U_s calculated for all the tests varied between 0.65 and 0.77, with an average value of 0.7. These calculations indicated that U_g/U_s is an increasing, apparently linear, function of U_g (which is supported by measurements by Matsumoto et al. [43]); that U_g/U_s increases with decreasing particle size; and that the value of μ has no effect at the prevailing high values of voidage ϵ.

The results for λ_s for section 2 for 96 conveying tests are plotted in Fig. 14, against the Froude number based on the mean air velocity. A least-squares power curve fit gave the correlation:

$$\lambda_s = 0.77Fr^{-1.05} \quad (n = 96, r^2 = 0.39) \quad (7)$$

This association of the average values of λ_s with the average values of Fr is somewhat unsatisfactory, bearing in mind that the variation in Fr along section 2 in a typical test was as great as the complete Fr range plotted in Fig. 14, but there is little alternative given the experimental circumstances. For purposes of comparison, a line showing the correlation by Konno and Saito [44] (but with a numerical constant twice as high, as recommended by Leung and Wiles [45]) is also plotted in Fig. 14.

It is of interest to compare the solids friction factors obtained for downward vertical flow with those obtained for horizontal flow. Fig. 15 shows the respective correlations obtained for one series of 30 tests (the same series as used for Fig. 4) during which the air vent was closed and the same air flow rates therefore applied in each test to both the horizontal section 1 and the vertical section 2. The vertical solids friction factors are seen to be less than those for horizontal flow throughout the range of flow rates tested (for U_g greater than 15.8 m/s).

There is little published information on co-current downward vertical flow (standpipe flow) with which Figs. 14 and

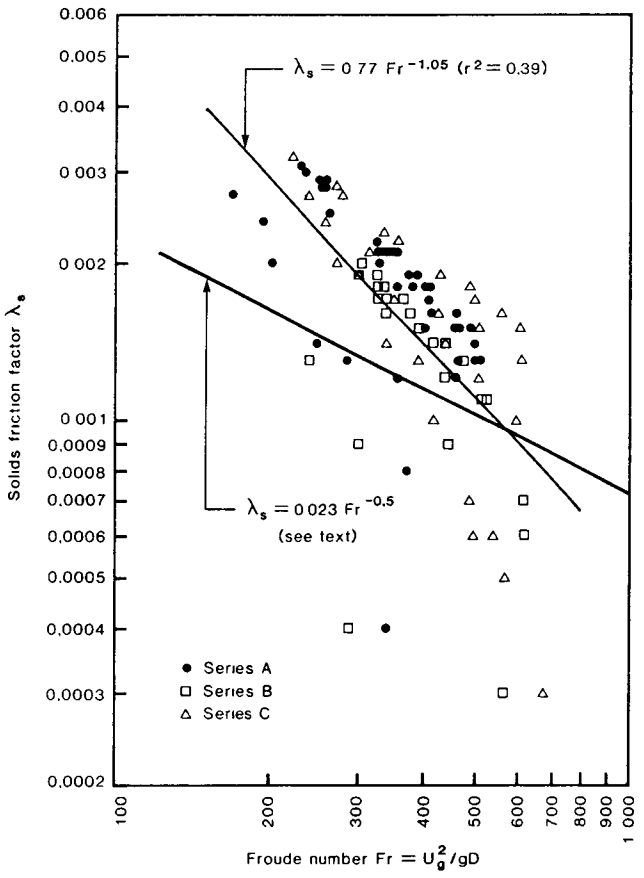

Fig. 14. Solids friction factors for downward vertical flow plotted against average Froude number.

15 can be compared. Leung [46] seems to suggest that correlations for upward vertical flow may also be used for downward dilute-phase flow and, if this is valid, there are many published correlations that could be considered. Leung and Wiles [45], Leung [46], Klinzing [47] and Klinzing et al. [37] have reviewed many of these and the most commonly recommended correlations are those by Konno and Saito [44] and, to a lesser extent, Yang [42]. Konno and Saito carried out conveying experiments with glass and copper beads and seeds ($d = 0.1$ to 1 mm) in 27 and 47 mm diameter glass pipes. Fig. 14 shows that the modified [45] version of the Konno and Saito correlation would give values roughly similar to those measured in this project. Leung [46] comments that neither Konno and Saito nor Yang took the coefficient of friction between particle and wall into account in their solids friction factor correlations, and cautions against extrapolating their correlations because of this 'serious omission'. The relative closeness of the two correlations in Fig. 14, in spite of the very low coefficient of friction between wet ice and plastic (overlooking the very different particle sizes involved), seems to show that the wall friction may not in fact be a decisive factor in this type of flow.

Of other researchers who have investigated co-current downward dilute-phase flow, McDougall [38] presented a simplified theoretical model (ignoring air compressibility) for predicting pressure gradients. The model did not extend to the prediction of induced air flow rates. Linear pressure profiles down a pipe were predicted and some limited experimental data from a small-scale rig seemed to bear this out. The data also indicated that the pipe-friction term in the model had little importance. He emphasized that further theoretical and experimental work would be required for a quantitative understanding of such flows, but this seems not to have eventuated. Stinzing [39] and De Jong [40] carried out limited small-scale experimental work, the latter postulating that the solids friction factor may be independent of pipe diameter. Kim and Seader [48] investigated pressure drop for suspensions of air and glass beads ($d = 0.33$ mm) flowing co-currently downwards in a short 13 mm diameter stainless-steel tube. They found that the frictional pressure drop in downflow was smaller than that in upflow, but the explanation given (recirculation of fine particles at the wall in upflow) would imply that this difference would not be present with large particles.

Various publications deal with the prediction of flow characteristics in standpipes, including those by Leung [46] and Chen et al. [49]. The latter described a model that takes compressibility into account but neglects wall friction in the dilute-phase region. The predictions were compared with measurements from a small test apparatus (standpipe length 3.27 m). Using coarse sand, the measured pressure profiles were found to be linear down the length of the pipe and this agreed with the predictions. Finally, Marjanovic et al. [23]

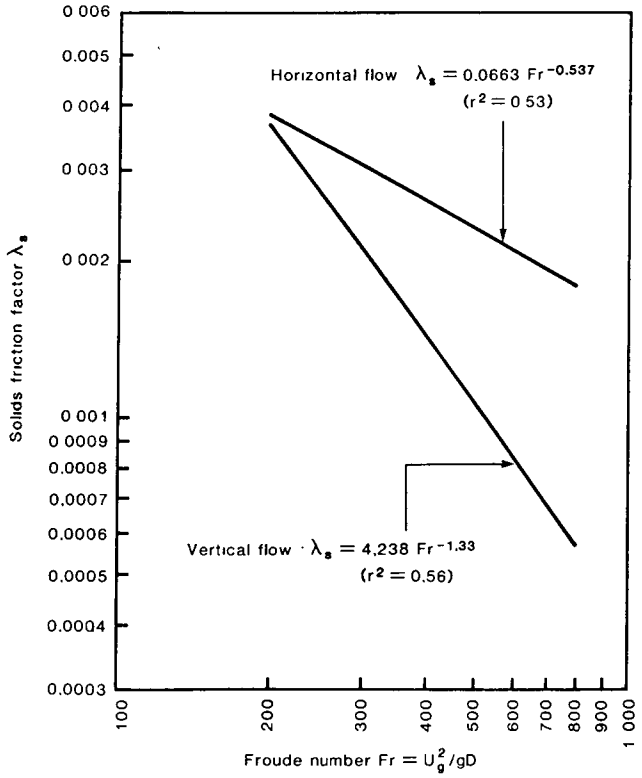

Fig. 15. Comparison of solids friction factors for vertical and horizontal flow, for one series of tests.

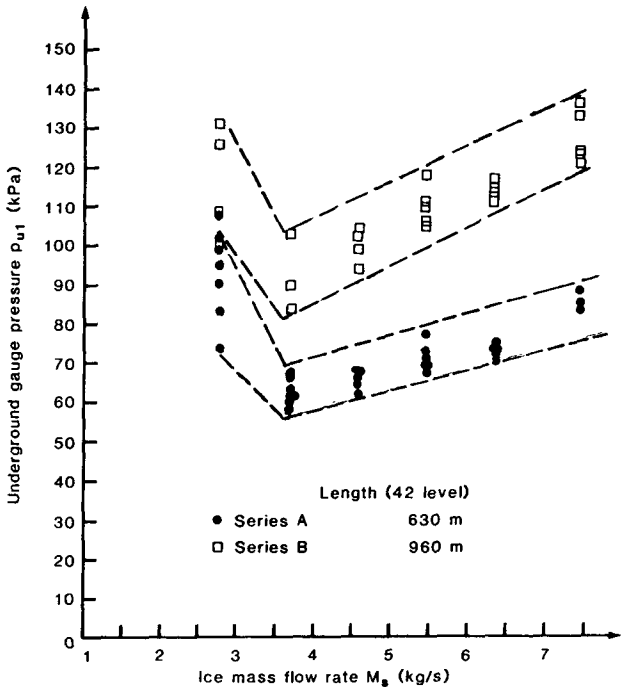

Fig. 16. Pressure drop along horizontal pipeline on 42 level at various ice flow rates (surface vent valve open).

carried out an experimental investigation into the conveying of various fine powders through 56 m long steel pipelines ($D=53$ and 81 mm) that included 16 m downward vertical sections followed by horizontal sections. Much of the testing programme was carried out with dense-phase flow, but aspects of the flow behaviour were notably similar to those observed in this ice project. As would be expected from an inspection of Eq. (4), they found that there could be either a small pressure drop or a pressure rise along the downward vertical section, depending upon the mass flow ratio. The profiles were approximately linear. Plugs formed after the bend at the bottom of the vertical section, because the air velocities were below the pickup values for suspension flow at that point, because of the rise in pressure.

6.3. Horizontal flow through pipe section 3

There were three independent variables governing the flow through pipe section 3: the pipeline length, the ice flow rate and the air flow rate. The air flow rate was controlled during one series of tests when the air vent on surface was closed, but in two other series of tests with an open vent the air flow was free to assume a value. The mass flow ratio μ varied between 3.5 and 20.4 in this pipe section. The superficial air velocity at the inlet to the section varied between 8.6 and 17.0 m/s with an open vent, while the range increased (10.2 to 22.6 m/s) with a closed vent.

Fig. 16 shows the underground gauge pressure measured at the foot of the vertical column (equal to the total pressure loss along section 3) plotted as a function of the ice flow rate, for tests with the vent on surface open. As the ice flow rate was increased from the lowest value of 2.76 kg/s the pressure at first decreased sharply and then, after passing through a minimum value at a flow of approximately 3.6 kg/s, increased gradually. Between these two flow rates there was a change from plug flow to loose slug flow, detectable from the downstream pressure fluctuations (e.g. Fig. 6), as mentioned previously. The range of measured pressures on this graph at a given ice flow rate, for either pipeline length, presumably reflects the (relatively small) variation in the quantity of air accompanying the ice, but no clear empirical correspondence could be discerned.

With the air vent closed the transition from plug to slug flow occurred less sharply, at flow rates of between approximately 4 and 6 kg/s, depending upon the respective air flow rates. It seems likely that the pipeline pressure drop would increase steadily thereafter with increasing ice flow rate, similarly to Fig. 16. At the lower (pre-transition) ice flow rates at which the closed-vent tests were mostly carried out, when full plug flow prevailed, it was found that the pipeline pressure drop increased with ice flow rate up to a peak value just before the transition, with a drop to a minimum after the transition. This behaviour is not apparent in Fig. 16 because flow rates lower than 2.76 kg/s were not investigated, but would be expected also to have applied in that case.

Of the few published analytical approaches to cohesive loose-plug (slug) conveying through long horizontal pipes, the most relevant for ice plugs is that by Muschelknautz and Krambrock [50]. This has been discussed in detail by Konrad [18,51] and by Dixon [52], who recommends the resulting expression for dense-phase design purposes, as do Wypych and Arnold [53]. This model yields the pipeline pressure loss by summing the pressure drops across individual one-dimensional plugs, in which there are no significant radial wedging forces, taking into account air compressibility along the pipeline. Muschelknautz and Krambrock made two significant assumptions: that the air friction loss through the pipeline is negligible and, more important, that the ratio U_s/U_g remains constant along the pipeline. The resulting expression for the solids pressure loss along the pipeline is:

$$\Delta p_s = p_0[\exp(\beta\mu gL/RTC) - 1] \tag{8}$$

where p_0 is the absolute pressure at the pipe exit and $C = U_s/U_g$. To take into account air friction it is assumed here that the air friction loss, given by the air-only version of Eq. (2), may be superimposed upon the solids pressure loss. Eq. (9) is the resulting expression for the absolute pressure p_1 at inlet to pipe section 3, where p_0 is the exit pressure:

$$p_1 = (p_0^2 + \lambda_g M_g^2 RTL/DA^2)^{1/2} + p_0[\exp(\beta\mu gL/RTC) - 1] \tag{9}$$

Using the ice-conveying measurements and the measured value of the friction coefficient β of 0.020 it was possible to calculate the value of the only unknown in Eq. (9), the average velocity ratio C, for each of 98 tests. The resulting values of C were plotted against the mass flow ratio μ, which

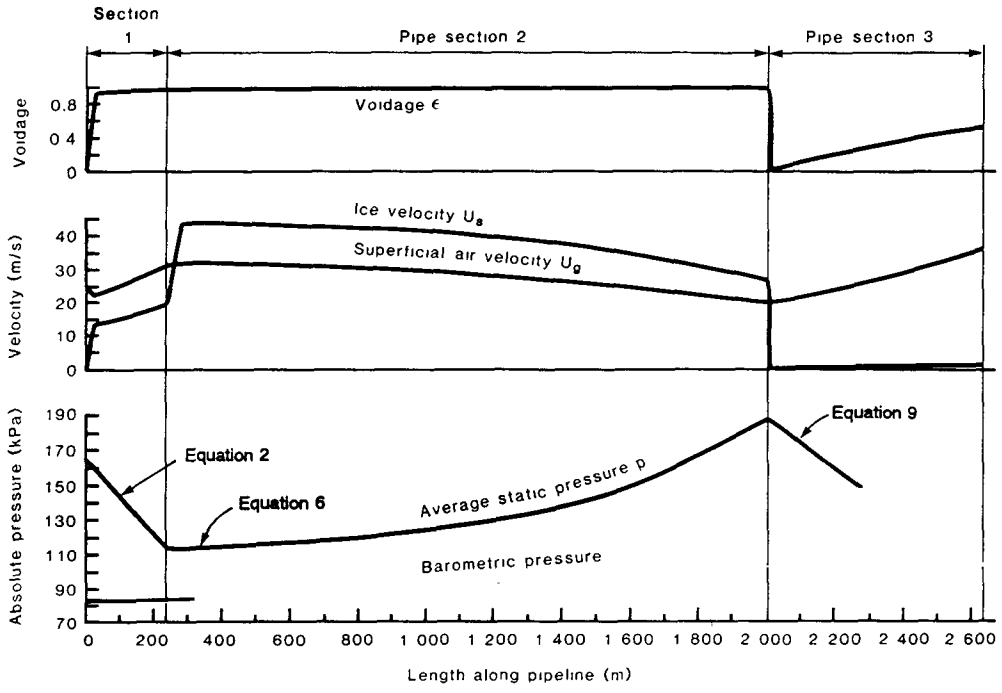

Fig. 17. Predicted profiles of pressure, air velocity, ice velocity and voidage along complete pipeline to 42 level for test C-32.

is indicated in the above-mentioned publications to be the most influential parameter affecting the value of C. A linear relationship was found to apply, with a fairly high coefficient of determination:

$$C = U_s/U_g = 0.003\mu \quad (r^2 = 0.83) \tag{10}$$

This relationship covered values of μ from 3.5 to 20.4 and no significant distinction was found between tests at low ice flow rate and those at high flow rate, or between tests with a 630 m section length and those with a 960 m length.

Insufficient experimental data were available to examine the important assumption that the velocity ratio C remains constant along the pipeline. Velocity ratio measurements (using high-speed photography) were limited to one position midway along section 3; 22 values were obtained during two conveying tests. The plug velocities, lengths and interplug separations varied substantially (the velocities by 30% about the mean values) and there was no discernible relationship between plug length and velocity. From these measurements the average velocity ratio at that position was $C = U_s/U_g = 0.013\mu$, a value more than four times higher than the overall value for the pipeline given by Eq. (10). A further observation of inconsistency is that the change in overall pressure loss with ice flow rate (Fig. 16) is not catered for by Eq. (9), if C is taken to be proportional to μ. The relationship obtained by substituting Eq. (10) into Eq. (8) implies that, for a given coefficient of sliding friction β and a given air temperature, Δp_s depends solely upon the pipeline length.

Further research would clearly be required to develop a more accurate model for this type of dense-phase flow. For practical purposes, however, the Muschelknautz–Krambrock model as expressed by Eq. (9) gives a sufficiently accurate basis for ice-conveying system design, using the average value for C given by Eq. (10). This model appears to provide a good basis for scaling to other pipeline lengths (strictly 'equivalent' lengths, to cater for bends). The question of scaling to different pipe diameters, however, remains unanswered; this simple loose-plug model is essentially independent of D.

7. Conclusions

This pilot-plant investigation proved the feasibility of conveying ice underground through long pipelines. An ice system of 29 MW cooling capacity has since been commissioned at East Rand Proprietary Mines Ltd. [12] and a pilot pneumatic-conveying system similar to that described here has operated successfully with slurry ice at another mine [4].

By using the models and correlations described, the pressure and velocity profiles along a complete ice-conveying pipeline may be estimated. As an example, Fig. 17 shows the resulting profiles for one test (C-32), the measured points for which appear in Fig. 9. These models have also been incorporated into a computer program to facilitate system design studies.

The largest remaining uncertainty in ice-conveying system design concerns the scaling of the present test results to pipes of different diameters, taking into account any associated changes in flow regime boundaries. Further research into the effect of pipe diameter on the conveying characteristics of large particles is required, for each of the types of flow observed in the respective pipe sections in this project. Wypych and Arnold [53] have discussed procedures for

scaling-up conveying characteristics obtained from pilot installations. They show that a general scaling model, for constant values of the gas mass velocity M_g/D^2 and the solids friction pressure drop Δp_s in each of two systems '1' and '2', is

$$\frac{M_{s2}}{M_{s1}} = \frac{\lambda_{s1}}{\lambda_{s2}} \frac{\rho_{g2}}{\rho_{g1}} \frac{L_1}{L_2} \left(\frac{D_2}{D_1}\right)^3 \quad (11)$$

Using the correlations for λ_s given in Eqs. (3) and (7) for horizontal flow (section 1) and vertical flow (section 2), respectively, the respective scaling-up equations may readily be obtained. These indicate ice flow rates proportional to $D^{2.5}$ in a horizontal pipeline such as section 1 and to $D^{1.95}$ in a vertical pipeline such as section 2. However, these relationships must clearly be regarded as tentative at this stage. For the plug or slug flow that was observed underground in section 3 the model adopted here does not give a sufficient basis for pipe diameter scaling and a different approach would seem to be required when future work is carried out.

8. List of symbols

a	factor defined by Eq. (6) (Pa^2)
A	cross-sectional flow area of pipe (m^2)
C	velocity ratio (U_s/U_g)
d	particle equivalent diameter (m)
D	pipe inner diameter (m)
Fr	Froude number (U_g^2/gD)
g	acceleration due to gravity (m/s^2)
L	length of section of pipeline (m)
M	mass flow rate (kg/s)
p	pressure (Pa)
r^2	coefficient of determination
R	specific gas constant (kJ/(kg K))
T	absolute temperature (K)
U	velocity (m/s)

Greek letters

β	coefficient of sliding friction
ϵ	void fraction of two-phase flow
λ	friction factor, Eq. (1)
μ	ice/air mass flow ratio (M_s/M_g)
ρ	density (kg/m^3)

Subscripts

f	due to friction
g	gas
s	solids
tot	total
z	due to vertical height
0,1,2	positions along pipeline

Acknowledgements

This paper arises from work carried out as part of a former research programme of the Chamber of Mines of South Africa. The author wishes to acknowledge the great assistance provided by the management and staff of East Rand Proprietary Mines Ltd., as well as the contributions made by his former colleagues at the Chamber of Mines Research Organisation, particularly R.M. Correia, E.J. Chaplain and W. Schmitz.

References

[1] T.J. Sheer, P.F. Cilliers, E.J. Chaplain and R.M. Correia, *J. Mine Vent. Soc. S. Afr., 38* (1985) 56.
[2] *ASHRAE Handbook: Refrigeration Systems and Applications*, ASHRAE, Atlanta, GA, 1986, Ch. 33.
[3] R.M. Correia, T.J. Sheer and E.J Chaplain, *J. Pipelines, 6* (1987) 155.
[4] R. Ramsden and F. Lloyd, *Proc. 5th Int. Mine Vent. Congr.*, Mine Ventilation Society, Johannesburg, South Africa, 1992, pp. 229–235
[5] T J. Sheer, *Ph.D. Dissertation*, University of the Witwatersrand, Johannesburg, 1991.
[6] H.H.G. Jellinek, *J. Colloid Interface Sci., 25* (1967) 192.
[7] P.V. Hobbs, *Ice Physics*, Clarendon Press, Oxford, 1974.
[8] A D. Roberts and J.D. Lane, *J. Phys. D: Appl Phys., 16* (1983) 275
[9] A Ahagon, T. Kobayashi and M. Misawa, *Rubber Chem. Technol., 61* (1988) 14.
[10] D.N. Mazzone, G.I. Tardos and R. Pfeffer, *Powder Technol., 51* (1987) 71.
[11] F.P. Bowden, *Proc. R. Soc. London, Ser. A, 217* (1953) 462
[12] R. Hemp, *Proc. 4th Int. Mine Ventilation Congr.*, Australian Institute of Mining and Metallurgy, Brisbane, Australia, 1988, pp. 415–423.
[13] A.R. Reed and S.R. Kessel, *Proc. 3rd Int. Conf. Pneumatic Conveying Technology, Pneumatech 3, Jersey, Channel Islands, 1987.*
[14] A.R. Reed and J.S. Mason, *Proc. 1st Int. Conf. Pneumatic Conveying Technology, Pneumatech 1, Stratford-upon-Avon, UK, 1982.*
[15] C.-Y. Wen and H.P. Simons, *AIChE J., 5* (1959) 263.
[16] J.F. Richardson and M. McLeman, *Trans. Inst. Chem. Eng , 38* (1960) 257.
[17] P.R Owen, *J. Fluid Mech., 39* (1969) 407.
[18] K Konrad, *Ph.D. Dissertation*, University of Cambridge, 1981.
[19] O Molerus, *Chem Eng. Sci., 36* (1981) 1977.
[20] Y. Tsuji and Y. Morikawa, *Int. J. Multiphase Flow, 8* (1982) 329.
[21] R.G. Boothroyd, *Flowing Gas–Solids Suspensions*, Chapman and Hall, London, 1971.
[22] R.D. Marcus, L.S. Leung, G.E. Klinzing and F. Rizk, *Pneumatic Conveying of Solids*, Chapman and Hall, London, 1990.
[23] P. Marjanovic, D. Mills and J S. Mason, *Proc. 3rd Int. Conf. Pneumatic Conveying Technology, Pneumatech 3, Jersey, Channel Islands, 1987.*
[24] E.E. Michaelides and I. Roy, *Int. J. Multiphase Flow, 13* (1987) 433.
[25] J.A. Hitchcock and C. Jones, *Br. J. Appl. Phys , 9* (1958) 218.
[26] B.L. Hinkle, *Ph.D. Dissertation*, Georgia Institute of Technology, Atlanta, GA, USA, 1953.
[27] H.E. Rose and R.A. Duckworth, *Engineer, 227* (1969) 392.
[28] M. Weber, *Bulk Solids Handling, 2* (1982) 231.
[29] W. Barth, *Chem. Ing. Tech., 30* (1958) 171.
[30] A.M. Scott, *Proc. 4th Int. Conf. Pneumatic Transport of Solids in Pipes, Pneumotransport 4, Carmel-by-the-Sea, CA*, BHRA Fluid Engineering, 1978.
[31] G.E. Klinzing, C.A. Myler, A. Zaltash and S. Dhodapkar, *Powder Technol., 58* (1989) 187.

[32] Y. Morikawa, Y. Tsuji, K. Matsui and Y. Jittani, *Int. J. Multiphase Flow, 4* (1978) 575.
[33] H. Ito, *Trans. ASME D, J. Basic Eng., 82* (1960) 131.
[34] P. Schuchart, *Chem. Ing. Tech., 40* (1968) 1060.
[35] Engineering Equipment Users' Association, *Pneumatic Handling of Powdered Materials, Handbook No. 15*, Constable, London, 1963.
[36] K.-E. Wirth and O. Molerus, *Proc. 2nd Int. Conf. Pneumatic Conveying Technology, Pneumatech 2, Canterbury, UK, 1984.*
[37] G.E. Klinzing, N.D. Rohatgi, A. Zaltash and C.A. Myler, *Powder Technol., 51* (1987) 135.
[38] I.R. McDougall, *Inst. Mech. Eng. Symp. Fluid Mechanics and Measurement in Two-Phase Flow Systems, Leeds, UK, 1969.*
[39] H.-D. Stinzing, *Proc. 1st Int. Conf. Pneumatic Transport of Solids in Pipes, Pneumotransport 1, Cambridge, UK*, BHRA Fluid Engineering, 1971.
[40] J.A.H. De Jong, *Powder Technol., 12* (1975) 197.
[41] A. Haider and O. Levenspiel, *Powder Technol., 58* (1989) 63.
[42] W.-C. Yang, *Ind. Eng. Chem., Fundam., 12* (1973) 349.
[43] S. Matsumoto, H. Harakawa, M. Suzuki and S. Ohtani, *Int. J. Multiphase Flow, 12* (1986) 445.
[44] H. Konno and S. Saito, *J. Chem. Eng. Jpn., 2* (1969) 211.
[45] L.S. Leung and R.J. Wiles, *Proc. 3rd Int. Conf. Pneumatic Transport of Solids in Pipes, Pneumotransport 3, Bath, UK*, BHRA Fluid Engineering, 1976.
[46] L.S. Leung, *Proc. 1980 Int. Fluidization Conf., Henniker, USA*, Plenum, New York, 1980, p. 25.
[47] G.E. Klinzing, *Gas–Solid Transport*, McGraw-Hill, New York, 1981.
[48] J.M. Kim and J.D. Seader, *AIChE J., 29* (1983) 353.
[49] Y.M. Chen, S. Rangachari and R. Jackson, *Ind. Eng. Chem., Fundam., 23* (1984) 354.
[50] E. Muschelknautz and W. Krambrock, *Chem. Ing. Tech., 41* (1969) 1164.
[51] K. Konrad, *Powder Technol., 49* (1986) 1.
[52] G. Dixon, in G. Butters (ed.), *Plastics Pneumatic Conveying and Bulk Storage*, Applied Science Publishers, London, 1981.
[53] P.W. Wypych and P.C. Arnold, *Powder Technol., 50* (1987) 281.